Atmospheric Pollution Research 5 (2014) 789-795
Short Communication

Atmospheric Pollution Research

www.atmospolres.com

Observations of air quality on the outskirts of an urban agglomeration during the implementation of pollution reduction measures

Yang Sun [1], Junke Zhang [1], Yuepeng Pan [1], Yuesi Wang [1], Tingting Liao [2], Tao Song [1]

[1] *State Key Laboratory of Atmospheric Boundary Layer Physics and Atmospheric Chemistry (LAPC), Institute of Atmospheric Physics, Chinese Academy of Sciences, Beijing 100191, China*
[2] *Plateau Atmospheric and Environment Key Laboratory of Sichuan Province, College of Atmosphere Sciences, Chengdu University of Information Technological, Chengdu, 610225, China*

ABSTRACT

Based on observations at Heshan, a boundary area in the city agglomeration of the Pearl River Delta region in China, atmospheric pollutants such as $PM_{2.5}$, O_3, CO, SO_2, NO_Z, NO_2 and NO were monitored between the 12th and 29th November, 2010. Meteorological parameters, including temperature, humidity, dew point, air pressure, ultraviolet light, wind direction, and wind speed were also measured. By combining the meteorological parameters with the atmospheric pollutant data, we performed Positive Matrix Factorization (PMF) and ozone production efficiency (OPE) analysis to objectively understand the interrelations among the pollutants, as well as between the pollutants and the meteorological factors. During the observation period, there were various meteorological changes such as rainfall, cold air transit, and sunshine that created conditions for the formation or dispersal of pollutants. The study period coincided with the 16th Asian Games, during which time the government adopted strict measures to reduce the discharge of pollutants around the Pearl River Delta area. However, we still observed serious pollution of $PM_{2.5}$ and O_3, of which the highest value of $PM_{2.5}$ was 210 μg m^{-3} and the highest value of O_3 reached 117 ppb. At the same time, the high concentrations of CO, NO, NO_2, NO_Z, and SO_2 could not be cleared away with rainfall in such a short period of time. On the basis of PMF analysis, we found that three factors influence the air quality of this region: local biomass burning, secondary pollutants of regional transport, and high industrial pollutant emissions. According to OPE analysis, the O_3 pollution was mostly found to be VOC–sensitive but occasionally NO_X–sensitive for OPE values greater than 10.

Keywords: *Ozone, $PM_{2.5}$, PMF, NO_Z, OPE*

Corresponding Author:
Tao Song
☎ : *+86-1062022285*
🖷 : *+86-1062362389*
✉ : *suny@dq.cern.ac.cn*

Article History:
Received: 22 December 2013
Revised: 16 June 2014
Accepted: 17 June 2014

doi: 10.5094/APR.2014.088

1. Introduction

Poor air quality is a topical issue in China due to the rapid increase in industry, vehicle numbers, and pollutant transport. The Pearl River Delta region (PRD) is one of the most seriously polluted areas, and its air quality problems are characterized historically by high concentrations of primary pollutants, such as sulfur dioxide (SO_2) and nitrogen oxides (NOx) (Xiao et al., 2006; Chan and Yao, 2008). In recent years, due to poor air quality and visibility, secondary air pollutants, such as fine particles as well as ozone pollution, have drawn increasing attention (Lam et al., 2005; Hagler et al., 2006; Zhang et al., 2007; Cheng et al., 2008; Zheng et al., 2010; Huang et al., 2012; Liu et al., 2013). Levels of SO_2, total reactive nitrogen (NO_Y), carbon monoxide (CO) and volatile organic compounds (VOCs) all contribute to the formation of fine particulate matter ($PM_{2.5}$) and ozone (O_3) (Hidy, 2000; Zaveri et al., 2003; Pathak et al., 2011; Lamsal et al., 2013). The NO and NO_2 emissions from fossil fuel combustion will exist for less than one day before being oxidized by air to become NO_Z (NO_Z=NO_Y-NOx), HNO_3, PAN (peroxyacetyl nitrate) and other reactive oxidized nitrogen species (Berkowitz et al., 2001; Jiang and Fast, 2004; Volz–Thomas et al., 2005; Horii et al., 2006; Raivonen et al., 2009). Previous studies have shown that $PM_{2.5}$ contains high concentrations of NO_Z (He et al., 2001; Pathak et al., 2004; Pathak and Chan, 2005; Pandey et al., 2006; Sillanpaa et al., 2006; Lee et al., 2008; Pathak et al., 2011).

Therefore, a part of $PM_{2.5}$ will be generated during the formation of O_3 in the photochemical reaction of NO_X and VOCs (Seigneur, 2001), which has not been analyzed in previous studies in the PRD. In the present study, observations were made in Heshan, the boundary area of the PRD city agglomeration, of atmospheric pollutants including $PM_{2.5}$, O_3, CO, SO_2, NO_Z, NO_2 and NO between the 12th and 29th November 2010. NO_Z concentrations were obtained by subtracting NO and NO_2 from observed NO_Y. Meteorological parameters, such as temperature, humidity, dew point, air pressure, ultraviolet light, wind direction and wind speed were also measured. A series of analyses regarding the whole set of meteorological and air quality data were performed, including Positive Matrix Factorization (PMF) and ozone production efficiency (OPE) analysis, so as to understand the changes and interrelations among the pollutants, as well as between the pollutants and meteorological parameters, when strict controls on pollutant discharges were imposed in this region.

These controls were introduced because, during the observation period, the 16th Asian Games were being held in Guangzhou, the largest city in the PRD region, 30 km away from the observation station. The Guangzhou Asian Games provided us with a unique opportunity to investigate the potential for pollution reduction in the PRD. The occurrence of this major sporting event condensed a comprehensive air quality management plan into a short–term aggressive abatement, revealing the possible improvements in air quality that can be made against a background of comprehensive environmental control measures (Liu et al., 2013).

2. Methods

The research site is located at the Heshan National Field Research Station in the forest ecosystem of the Chinese Academy of Sciences, which lies in the central region of Guangdong Province (112°53'E, 22°40'N). This experimental area features many low, gentle hills and a mild climate with an average annual temperature of 21.7 °C and maximum and minimum temperatures of 29.2 °C and 12.6 °C, respectively. The height of the sampling point was approximately 45 m above sea level, and located 34 km southwest of Guangzhou and 20 km and 30 km away from Foshan and Jiangmen, respectively (see the Supporting Material, SM, Figure S1). The predominant wind direction in the fall is from the northeast (see the SM, Figure S7). Because a high concentration zone tends to form approximately 30 to 80 km from an emission source by remote transmission and evolution of atmospheric photochemical pollutants, Heshan is in a good location to observe the pollutant levels in an atmospheric smoke plume from surrounding cities.

The O_3 and NO_Y analyzers were Model 49i and Model 42Y (Thermo Environmental Instruments Inc., USA); while for NO and NO_2, Model CLD 88 and Model PLC 860 (ECO PHYSICS AG, Switzerland) were used. All analyzers were calibrated before the field campaign according to the standards of the Chinese Environmental Protection Bureau. The SO_2 and CO analyzers were Model 43i and Model 48i (Thermo Environmental Instruments Inc., USA) while the $PM_{2.5}$ mass concentrations over the station was measured using a Tapered–Element Oscillating Microbalance (TEOM) instrument with quartz filter (Pallflex TX40) and one record every two seconds and with an accuracy of ±1.5 μg m^{-3} for hourly averages, although it can underestimate $PM_{2.5}$ mass concentration owing to volatilization of ammonium nitrate and organic carbon (Gupta and Christopher, 2009). For the meteorological variables, the Milos520 (Vaisala, Finland) was used, which is an automatic, meteorological observation tower located at Heshan Station, and its observation parameters include air temperature, relative humidity, sea level pressure, and wind (Hu et al., 2010). The location of the present observation point complied with China Ambient Air Quality Standards II which requires 24–hourly average concentration limits of SO_2, NO_2, CO, and $PM_{2.5}$ respectively to be below 150 m^{-3}, 80 μg m^{-3}, 4 mg m^{-3}, 75 μg m^{-3} and 1–hourly average concentration of O_3 below 200 μg m^{-3}.

3. Results

3.1. Pollutants time series analysis

The mixing ratio curves of $PM_{2.5}$, O_3, CO, SO_2, NO_Z, NO_2 and NO are plotted as time series in Figure 1, while Figure S2 (see the SM) shows wind speed, temperature, relative humidity, dew, ultraviolet radiation, and air pressure for the observed period.

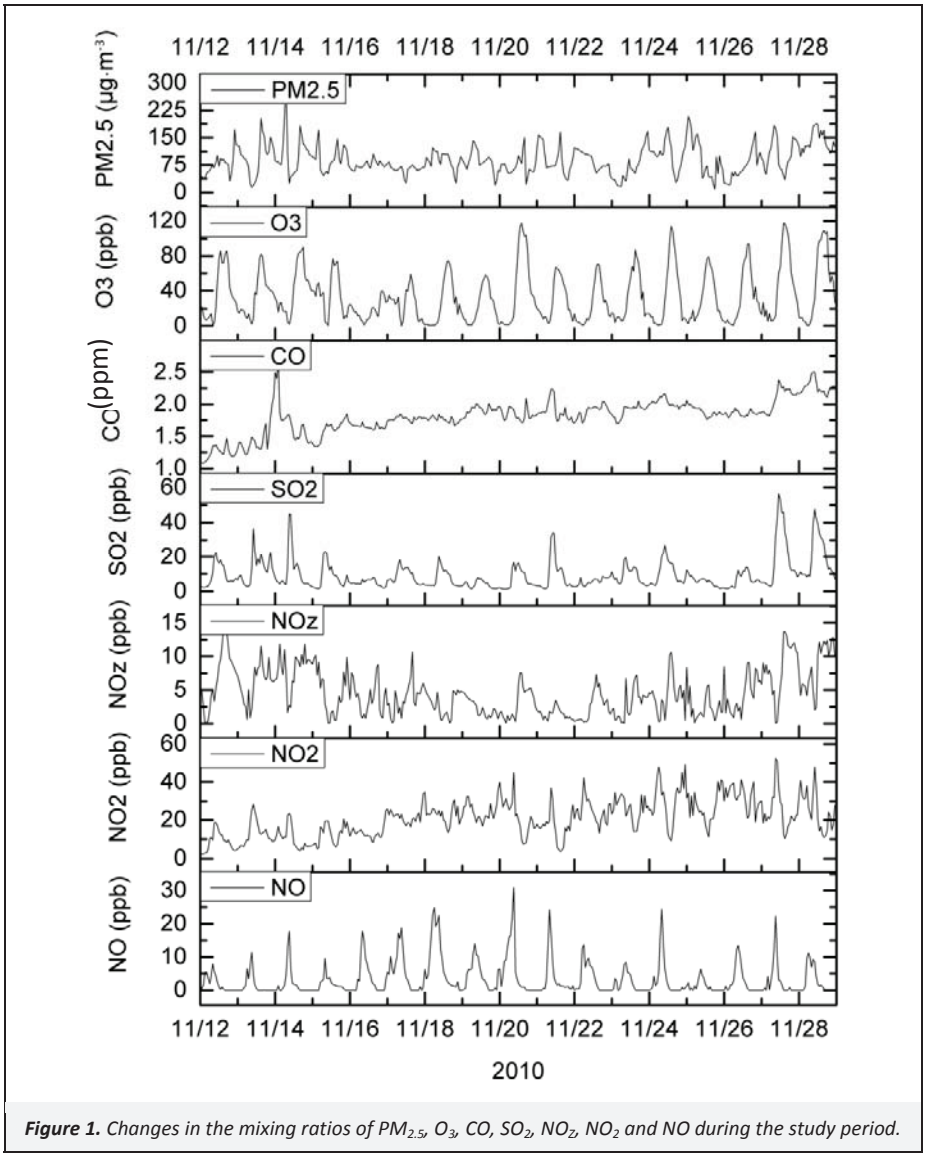

Figure 1. *Changes in the mixing ratios of $PM_{2.5}$, O_3, CO, SO_2, NO_Z, NO_2 and NO during the study period.*

The NO_2 concentration in the first stage was lower, but the mean concentrations of NO and NO_Z were higher. In the second stage, the mean concentrations of O_3, NO_Z, and NO_2 were higher, but the concentrations of NO and NO_Z were lower. The concentrations of O_3 exceeded 100 ppb on the 20th, 24th, 27th and 28th November. In particular, O_3 reached an hourly maximum value of 120 ppb in the observation period on the 20th November. Moreover, NO_Z reached their peak values in the observation period on the 27th; these peaks are analyzed in detail later in the paper. There is a good positive correlation between NO_Z and O_3 according to the Figures S4 and S6 showing the Factors 1 and 3 (see the SM). In Factor 2 (see the SM, Figure S5), there is a higher concentrations of NO, NO_2 and NO_Z, but the O_3 is not high, and it can be seen that $PM_{2.5}$ and relative humidity are rather high too, which indicates the meteorological factors and atmospheric chemical reactions related to Factor 2 are not in favor of O_3 production, but in favor of particle production on the contrary.

Therefore the rising of NO_Z concentration might probably be contributed by rising of nitrate, which is also one of the major components in particles. The particle nitrate as well as nitric oxide produced by photochemical reaction from other gaseous NO and NO_2 are contained in NO_Z, therefore, NO_Z has a good correlation trends with O_3 under the same weather conditions, with a large range of variation in concentrations.

The $PM_{2.5}$ concentration remained high during the entire observation period, and even reached 210 μg m^{-3} on the 13th (Figure 2). It showed irregular major fluctuations in the periods between the 12th and 15th and between the 22nd and 28th November. This kind of pulsation–type change is similar to the overall change of SO_2 and NO_Z, as well as to the pattern of temperature, but is the opposite of the change seen for NO. The high concentration of $PM_{2.5}$ during the period when pollutants were strictly controlled in the PRD region shows the severity of atmospheric contamination and the difficulties involved in pollutant control.

The concentration of CO showed the smallest level of change among all the pollutants, but it was still a major contaminant. The highest mean value per hour reached 2.5 ppm, when $PM_{2.5}$ reached its peak value of 210 μg m^{-3} which reflects the intensity of fossil fuel emissions in this region. There were two occasions when the concentration of SO_2 exceeded 40 ppb and the highest value of SO_2 in the region always occurred at noon of each day, when there is a full convection current in the atmospheric boundary layer. The reason may be that emissions of SO_2 in this region are mainly caused by elevated stacks of coal–burning plants, lifting the pollutant into the mixing layer so that it is mixed to the ground in the full convection current. In addition, the high concentration and regular changes of NO, which showed classic rush–hour related peaks, possibly arose from vehicle emissions of staff working at the observation station.

3.2. Pollution episode analysis

On November 20th, 2010, Heshan Station recorded serious photochemical pollution. The highest concentration of O_3 reached was 117.4 ppb in one hour, and the next day the $PM_{2.5}$ average one–hour concentration was 160 μg m^{-3}. Given the very high concentrations of these two kinds of pollutants on these two days, it was necessary to analyze the change process.

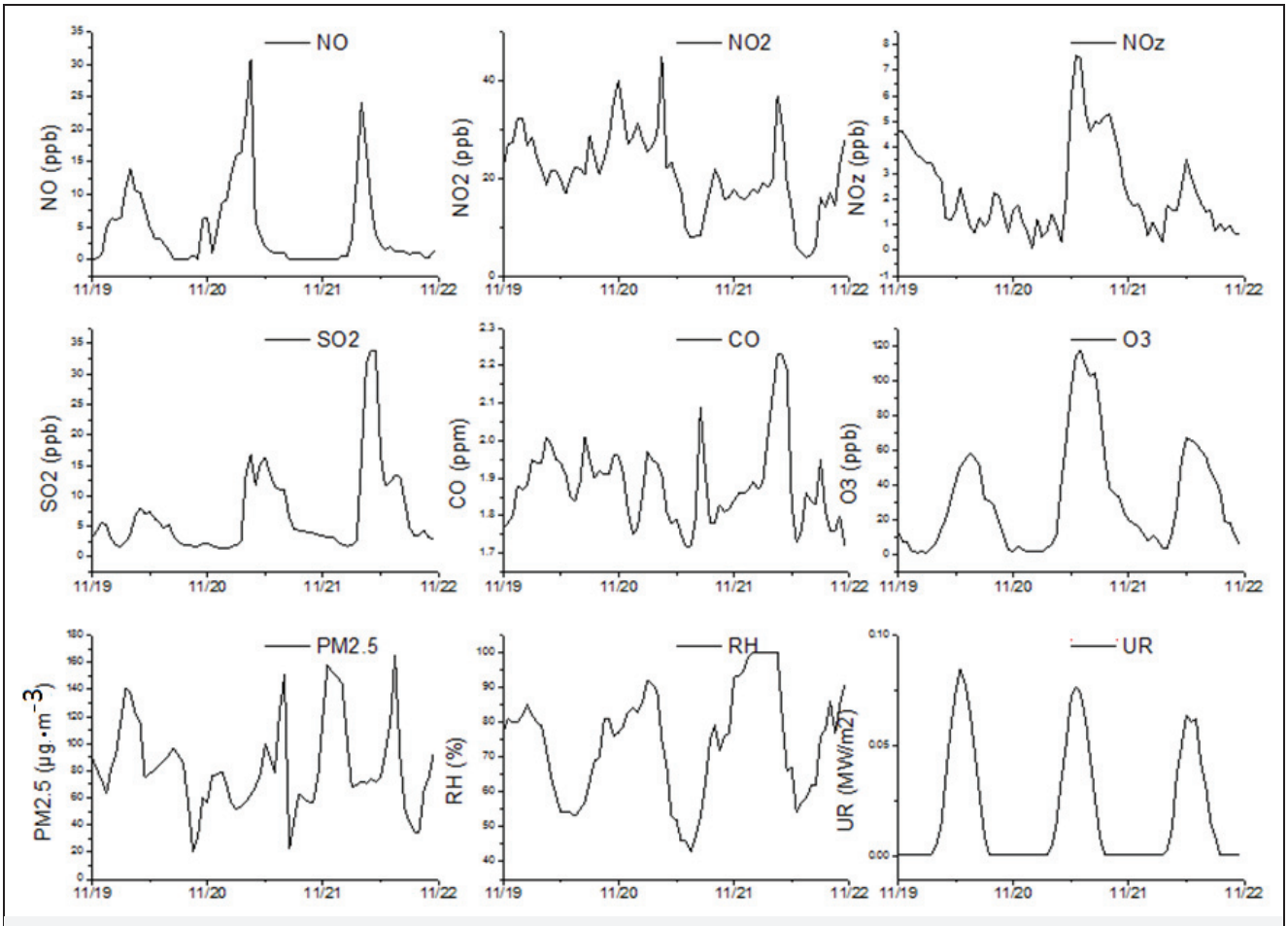

Figure 2. *Daily variations of $PM_{2.5}$, O_3, CO, SO_2, NO_Z, NO_2, NO, relative humidity, and ultraviolet radiation from November 19th to 21st.*

There were concentration peaks of $PM_{2.5}$ in the morning on the latter two days, and irregular changes during the evening. The fluctuations of $PM_{2.5}$ were more marked than O_3 fluctuations, and dissimilar to any meteorological factor. NO increased simultaneously with SO_2, but did not share the same range of increase. The peak value of SO_2 was more regular at 12:00 PM. There were corresponding local sources of pollution near the observation station, except for the elevated source of emissions and mixing on the ground due to the lifted mixing layers. There was rainfall lasting for several hours on the morning of the 21st, during which the relative humidity was as high as 100%. Thus, it can be seen that rainfall can inhibit the generation of O_3 and NO_Z as well as remove SO_2 and $PM_{2.5}$. However, the situation quickly returns to its previous state after the rainfall stops. Moreover, NO and CO are not affected by rainfall at all, and in fact accumulate more with rainfall due to inadequate dispersion.

It can be seen in Figure 2 that the concentration of NO was high after the morning of the 19th, and NO_2 accounted for a large proportion of the concentration. NO_Z decreased by 5 ppb at night. NO_2 also showed the same downward trend because of removal by dry deposition. NO concentration increased gradually after 6:00 AM to the daily maximum at 9:00 AM, which is typical for traffic emissions. O_3 concentration began to rise after 9:00 AM because of photochemical reactions. However, ultraviolet radiation reached its highest value within the three days. The wind speed increased to 4 m s^{-1}, which helped transport of pollutants. Therefore, the hourly maximum mean value of O_3 could only reach 60 ppb. In addition, on the 19th, the wind speed decreased at dusk, the sustained temperature was higher, air pressure increased, and the boundary layer was stable, which helped NO_2 to accumulate to a maximum of 40 ppb at night. NO_2 continued to accumulate on the morning of the 20th starting at 3:00 AM. NO increased rapidly, and it reached a maximum of 30 ppb at 9:00 AM, which was higher than the previous day. NO_2 also increased noticeably. Furthermore, the addition of ultraviolet radiation caused the temperature to increase rapidly. The wind speed averaged 1.5 m s^{-1}, which mixed the precursors and facilitated atmospheric photochemical reactions. Humidity dropped to a minimum of 40%. These conditions were favorable for photochemical reactions. Therefore, NO and NO_2 concentrations were higher in the morning on the same days but very low at 2:00 PM, and the O_3 and NO_Z concentrations increased quickly and reached their maximum hourly mean values of 120 ppb and 7.5 ppb, respectively, at 2:00 PM. The model results appear consistent with the observed NO_Y, NO_Z and O_3 data. The high concentrations of pollution did not diffuse and clear until 6:00 PM. This process allowed O_3 to exceed 100 ppb for five consecutive hours. O_3 and NO_Z were cleared, and the concentrations were reduced by the dry deposition that occurred at night, but O_3 still remained at approximately 20 ppb from nighttime to the morning of the 21st. Then, traffic peaked again at 9:00 AM on the 21st, and NO and NO_2 showed remarkable peak values. However, the wind speed was almost zero because of lower ultraviolet radiation on that day, and the humidity increased to 100% after 4:00 AM. These meteorological conditions were unfavorable for photochemical reactions. Therefore, the maximum concentration of O_3 was only 65 ppb on the 21st, which is not a serious level of pollution. Thus, it can be observed that the high–concentration O_3 pollution event that occurred on the 20th was caused by weather conditions, such as stable weather, breeze, low humidity, and low pressure, in addition to high concentrations of NO_X emitted by peak traffic. The generation of O_3 accompanied the generation of NO_Z, which means that other oxidation products play a role in the generation efficiency of O_3. This effect is further analyzed in Section 3.4.

3.3. EPA PMF analysis

PMF is a multivariate factor analysis tool (Paatero and Hopke, 2009) that has been applied to a wide range of data, including $PM_{2.5}$ data, size–resolved aerosol data, deposition data, air toxicity data, and volatile organic compound (VOC) data (Poirot et al., 2001; Polissar et al., 2001; Kim et al., 2003; Kim and Hopke, 2004). PMF decomposes a matrix of ambient data into two matrices, which an analyst then interprets to identify the represented source types (Brown et al., 2012). Here, we use the U.S. EPA version, PMF 3.0, which has been widely applied in regulatory assessments since PMF 1.0 (Hegg et al., 2009). In the analysis of spatiotemporal data, factor analytic models have also been widely used in meteorology to analyze spatially distributed data. Recently, models based on the non–negatively constrained PMF approach have gained popularity (Paatero et al., 2003).

Three to six factor solutions were explored with EPA PMF 3.0, and 20 runs from a random seed were performed for each number of factors. Random starting seeds were used to increase the likelihood of finding a global minimum of the goodness–of–fit parameter, Q. We focus the remainder of the analyses on the three–factor solution.

In Factor 1, O_3 contributes significantly, accounting for above 80% (see the SM, Figure S4). In addition, NO_Z accounts for 70% of the factor, the value of $PM_{2.5}$ is up to 30%, and the load of meteorological factor UV is up to 80%. All these values mean that the pollution of Factor 1 possesses oxidizability and is the product of photochemical reactions, especially NO_Z coming from the generation of O_3, which will be discussed in detail in Section 3.5 on OPE (NO_X) analysis. Besides, those values also prove that some part of $PM_{2.5}$ is generated from photochemical reactions. In Factor 1, SO_2 also contributes significantly, accounting for 60%, and CO accounts for 30%. This means that, in this factor, there is primary pollution generated from combustion. Furthermore, wind speed accounts for almost nothing, meaning that the primary pollution comes from local sources, which relates to straw–burning and power plant emissions in this season.

Regarding Factor 2 (see the SM, Figure S5), NO, NO_2, NO_Z, CO, and $PM_{2.5}$ contribute significantly, and the loads of each of factors exceed 50%. The main contributors in terms of the meteorological factors are temperature, humidity, dew point and air pressure. The main pollutants emitted from the gasoline–fueled vehicles that are related to high loads of this factor are NO, NO_2, and CO, but the direct emissions of $PM_{2.5}$ are fewer, because the emissions of diesel vehicles are mainly NO, NO_2, NO_Z, CO, SO_2 and $PM_{2.5}$. In terms of meteorological factors, wind speed and ultraviolet light have little relation with Factor 2. Therefore, long–range transport need not be considered. The contribution of the ultraviolet radiation is very low, indicating that it is cloudy or in nighttime. The photochemical reaction products are very low and ozone concentrations are low. We think this part of the pollutants were primary pollutants. The main component of $PM_{2.5}$ and NO_X and CO, the peak in the early morning (see the SM, Figure S5), which is consistent with the time of vehicle driving behavior and the exhaust emissions. Factor 2 is mainly related with primary pollutants and secondary generation from vehicle emissions.

According to the pollutants' contributions in Factor 3 (see the SM, Figure S6), it can be seen that NO and NO_2 are the main contributors to the distributions of Factor 3, accounting for 60% and 40%, respectively. This means that NO has a greater relevance for Factor 3 but does not mean that there is a high concentration of NO. Other pollutants contribute less in Factor 3, and wind speed contributes significantly among all the meteorological parameters. This means that the factor represents the atmospheric background under good dispersion conditions and the regional status across a wide range. Pollution of the air mass under this background is mainly in the form of NO_X, which may be related to pollution emission restrictions in the PRD region. This is also consistent with the literature insofar as the effect of mitigating SO_2 is more obvious than that of NO_X (Chen et al., 2010; Liu et al., 2013; Xu et al., 2013; Zhang et al., 2013).

In terms of Factor 3, there is some CO and SO_2 present, which are primary pollutants in the background atmosphere. Furthermore, there is almost no O_3 and $PM_{2.5}$ in the background atmosphere; plus, there is obvious reduction for the pollution. In the PRD region, there are two sources for NO_X in the atmosphere, including mobile sources from vehicle emissions and stationary sources from thermal power generation, industrial production, and burning of fossil fuels. As the amount of vehicles in urban areas is increasing rapidly, there is more and more NO from mobile sources. SO_2 in the regional atmosphere mainly comes from combustion sources, while coal combustion and emissions from diesel vehicles are the main sources of SO_2. It can be concluded that Factor 3 represents pollution from local combustion sources, and the proportion of SO_2 is smaller than that of NO_X. Therefore, Factor 3 comes from vehicle emissions. Although the linear curve fit between NO_Z and O_X has poor coefficient of correlation according to the data, the trend indicated is consistent with the Factor 3.

According to the PMF analysis results of the 3 factors above, the gaseous and particulate pollutants of the sampling sites came from three factors mainly.

The profiles of three main factors are defined respectively as, (1) primary coal combustion and photochemical pollutants, (2) primary pollutants and secondary pollutants formed by multiphase reactions, and most of the process is the moisture absorption of particles, and (3) primary pollutants from vehicles and biomass combustion emissions in majority. The concentration of pollutants by Factor 1 is highest among the 3 factors, contributing most pollutants in the area, with a regular diurnal variation of high in day and low at night. The pollutants due to Factors 2 and 3 are almost equal to each other. Factor 2, presents a regular diurnal variation as Factor 1, with a phenomenon of high concentrations during night and early in the morning and low concentrations during the daytime. Factor 3 does not seem to have an obvious diurnal variation, but there is a close relation with wind speed, which represents the character of the area. So it could be concluded that, PMF model cannot only be used to the research on sources of pollutants, but also is a powerful tool in extensive analysis on air pollution.

3.4. OPE (NO_X) analysis

The NO_X acts as the catalyst and plays a role of circulation in the process of O_3 production in the atmospheric photochemical reactions, in which, however, the NO_2 will be oxidized to nitric acid by OH, and then the nitric acid will be removed from the atmosphere through further deposition. Therefore, OPE is a good indicator in characterizing the ability of generating O_3 by NO_X and VOCs, which can also evaluate the causes of the generation of O_3 and become the theoretical basis of O_3 control strategies. At the same time, due to the fact that the OPE can be obtained through a model calculation, so that it can be obtained by observations (Chou et al., 2009), it can be a good indicator of the validity of the simulation.

OPE can be calculated through ozone and NO_Y or NO_X data measured directly. A feasible formula has been established based on observations, and the calculation result can be used for analyzing the sensitivity of ozone. There are many forms of the formula of OPE, but the experimental results showed that the NO_2 photolysis in daytime can generate O_3 rapidly, and therefore there exists a significant linear relationship between O_3 and NO_X, as well as O_3 and NO_Y; the NO_Z here refers to HONO, HNO_3, PAN, and other nitrogen oxides. OPE can be defined as $\Delta(O_X)/\Delta(NO_Z)$ (Trainer et al., 1993; Nunnermacker et al., 1998).

NO_Z from the oxidation product of NO_X, and the mixing ratio of NO_Z, will increase with the increasing amount of O_3 generated. The quantitative relation between the NO_Z concentration and the increase of O_X ($O_X=O_3+NO_2$) concentration can be used to calculate the daily OPE value, and the OPE values were determined by the concentration relation between O_X and NO_Z fitted from 08:00 AM to 13:00 PM in this study. Ozone production efficiency (OPE) refers to the number of O_3 molecules generated by consuming an NO_X molecule in the atmospheric photochemical reactions.

The high–ozone pollution cases on November 20th and 27th are the examples of this method. Figures 3a and 3b respectively show that there is an obvious positive correlation and linear relationship between O_X and NO_Z during these two days. The slopes show that the averages of OPE were 11.8 and 3.9 ppb/ppb in these periods, respectively. There were obvious differences in OPE values obtained during these two days.

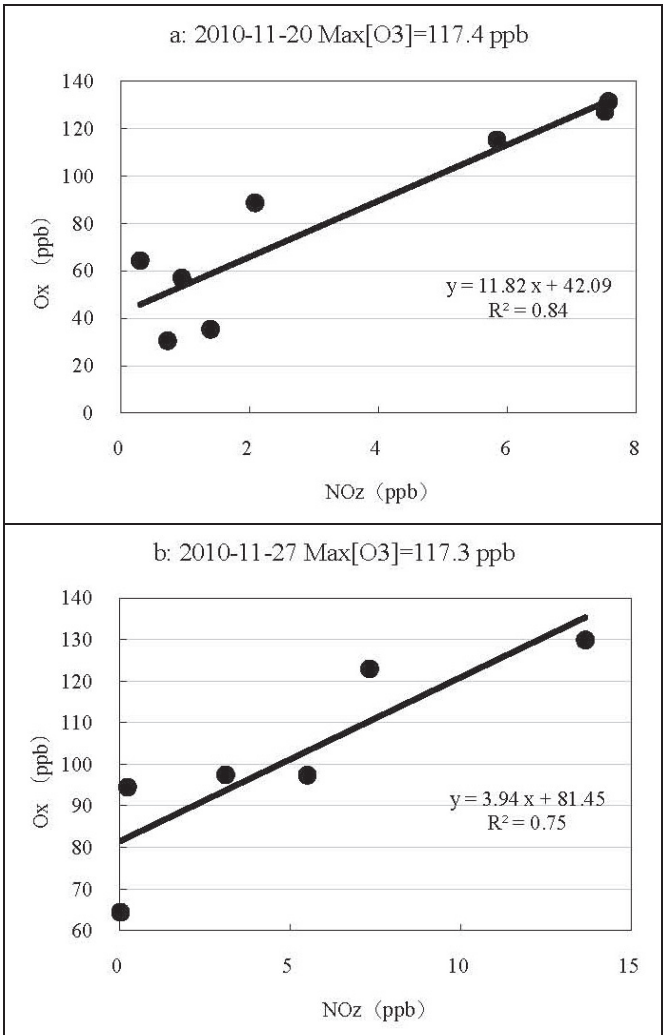

Figure 3. *OPE obtained from the regression equation of $\Delta(O_X)/\Delta(NO_Z)$:* ***(a)*** *November 20th, 2010;* ***(b)*** *November 27th, 2010.*

The OPE values in the previous studies ranged largely from 10 in the population source area to greater than 100 in the clean area; some of those values were obtained from observations and others from simulated calculations (Stehr et al., 2000; Berkowitz et al., 2004). The values of OPE found in the present study are consistent with the results in the literature.

Observed values also have many other differences, such as the concentrations of NO_X and VOCs, UV, RH, air temperature, and so on. Meanwhile, the significant change reflected by the different typical regions also proved that the OPE is able to demonstrate the impact of the transfer of pollutants by air masses, and the NO_X is constantly being oxidized via photochemical aging or air mass processes. This reduces its concentration in the system, and the

system shifts from being VOC–dependent to NO_X–dependent, which generates O_3 in polluted areas. In this study, OPE increased over the study period, and a high mixing ratio ozone pollution episode usually appeared in downwind areas from the urban site, because ozone is continuously produced in the city smoke plume. The generation of O_3 transitioned from being VOC–dependent to NO_X–dependent, which is consistent with the conclusions of other studies (Roussel et al., 1996; Li et al., 1997).

We obtained OPE values through the linear fitting method in the observation period between 08:00 AM and 14:00 PM, and calculated the maximum mixing ratio of O_3 in one hour. The correlation is not directly between their concentrations data, because the O_3 concentration can reach the maximum not only by being related to O_3 formation efficiency at that time, but also by being controlled by the atmospheric chemical reaction relationship between the nonlinear precursors. A higher initial NO_X mixing ratio will lead to lower OPE following the reaction cycle during the O_3 formation process with the same conditions. OPE can indicate NO_X restriction or NO_X saturation. The paradigm has been established of the ratio of O_3 and NO_Z less than 7, which means VOC sensitivity in the O_3 production process (Sillman, 1995).

The OPE value was slightly greater than 10 on one high ozone day in our work, suggesting a transitional state and O_3 production in the region being NO_X–sensitive. On another day, the OPE value was far less than 10, meaning the generation of O_3 was strongly VOC–dependent and mostly generated from local photochemical reactions.

4. Conclusions

In the period from Nov. 12th to Nov. 29th 2010, $PM_{2.5}$, O_3, CO, SO_2, NO_Z, NO_2, and NO were observed at Heshan Station, which is located 34 km southwest of Guangzhou. The observations were made during the 16th Asian Games, at a time when the government had adopted strict measures to reduce the discharge of pollutants around the PRD area. However, we still observed serious pollution of $PM_{2.5}$ and O_3, of which the highest value of $PM_{2.5}$ was 210 μg m^{-3} and the highest value of O_3 reached 117 ppb. On the basis of PMF analysis, it was found that three factors influence the air quality in this region: local biomass burning, secondary pollutants of regional transport, and high industrial pollution emissions. The generation of high concentrations of O_3 accompanied the generation of high concentrations of NO_Z, of which the maximum was 14 ppb. According to the OPE analysis, most of the time the pollution of O_3 was VOC–sensitive and derived from regional photochemical pollution over shorter distances. OPE value was slightly greater than 10 on one high ozone day in our work occasionally, suggesting a transitional state and O_3 production in the region being NO_X–sensitive.

Acknowledgments

This study was funded by the National Natural Science Foundation of China (41175107 ,41275139 and 41230642) and the "Strategic Priority Research Program" of the Chinese Academy of Sciences (No. XDA05100100&XDB05020000). The authors thank Dongsheng Ji and Bo Hu for their valuable help with the methodologies employed in the study.

Supporting Material Available

Map of Heshan Station in Guangdong province (Figure S1), Time series of wind speed, wind direction, ultraviolet radiation, air pressure, dew temperature, relative humidity, and temperature during the observation campaign period (Figure S2), Weather map of 850 hPa in China (Figure S3), The profile and contributions of the first factor from the three–factor PMF results (Figure S4), The profile and contributions of the second factor from the three–factor PMF results (Figure S5), The profile and contributions of the third factor from the three–factor PMF results (Figure S6), The relationship between wind direction and the extent values (Figure S7). This information is available free of charge via the internet at http://www.atmospolres.com.

References

Berkowitz, C.M., Jobson, T., Jiang, G.F., Spicer, C.W., Doskey, P.V., 2004. Chemical and meteorological characteristics associated with rapid increases of O_3 in Houston, Texas. *Journal of Geophysical Research–Atmospheres* 109, art. no. D10307.

Berkowitz, C.M., Zaveri, R.A., Bian, X.D., Zhong, S.Y., Disselkamp, R.S., Laulainen, N.S., Chapman, E.G., 2001. Aircraft observations of aerosols, O_3 and NO_Y in a nighttime urban plume. *Atmospheric Environment* 35, 2395–2404.

Brown, S.G., Lee, T., Norris, G.A., Roberts, P.T., Collett, J.L., Paatero, P., Worsnop, D.R., 2012. Receptor modeling of near–roadway aerosol mass spectrometer data in Las Vegas, Nevada, with EPA PMF. *Atmospheric Chemistry and Physics* 12, 309–325.

Chan, C.K., Yao, X., 2008. Air pollution in mega cities in China. *Atmospheric Environment* 42, 1–42.

Chen, H., Wang, Z., Wu, Q., Wang, W., 2010. Source analysis of Guangzhou air pollutants by numerical simulation in the Asian Games Period. *Acta Scientiae Circumstantiae* 30, 2145–2153 (in Chinese).

Cheng, Y.F., Wiedensohler, A., Eichler, H., Su, H., Gnauk, T., Brueggemann, E., Herrmann, H., Heintzenberg, J., Slanina, J., Tuch, T., Hu, M., Zhang, Y.H., 2008. Aerosol optical properties and related chemical apportionment at Xinken in Pearl River Delta of China. *Atmospheric Environment* 42, 6351–6372.

Chou, C.C.K., Tsai, C.Y., Shiu, C.J., Liu, S.C., Zhu, T., 2009. Measurement of NO_y during Campaign of Air Quality Research in Beijing 2006 (CAREBeijing–2006): Implications for the ozone production efficiency of NO_x. *Journal of Geophysical Research–Atmospheres* 114, art. no. D00G01.

Gupta, P., Christopher, S.A., 2009. Particulate matter air quality assessment using integrated surface, satellite, and meteorological products: Multiple regression approach. *Journal of Geophysical Research–Atmospheres* 114, art. no. D14205.

Hagler, G.S., Bergin, M.H., Salmon, L.G., Yu, J.Z., Wan, E.C.H., Zheng, M., Zeng, L.M., Kiang, C.S., Zhang, Y.H., Lau, A.K.H., Schauer, J.J., 2006. Source areas and chemical composition of fine particulate matter in the Pearl River Delta region of China. *Atmospheric Environment* 40, 3802–3815.

He, K.B., Yang, F.M., Ma, Y.L., Zhang, Q., Yao, X.H., Chan, C.K., Cadle, S., Chan, T., Mulawa, P., 2001. The characteristics of $PM_{2.5}$ in Beijing, China. *Atmospheric Environment* 35, 4959–4970.

Hegg, D.A., Warren, S.G., Grenfell, T.C., Doherty, S.J., Larson, T.V., Clarke, A.D., 2009. Source attribution of black carbon in Arctic snow. *Environmental Science & Technology* 43, 4016–4021.

Hidy, G.M., 2000. Ozone process insights from field experiments – Part I: Overview. *Atmospheric Environment* 34, 2001–2022.

Horii, C.V., Munger, J.W., Wofsy, S.C., Zahniser, M., Nelson, D., McManus, J.B., 2006. Atmospheric reactive nitrogen concentration and flux budgets at a Northeastern US forest site. *Agricultural and Forest Meteorology* 136, 159–174.

Hu, B., Wang, Y.S., Liu, G.R., 2010. Long–term trends in photosynthetically active radiation in Beijing. *Advances in Atmospheric Sciences* 27, 1380–1388.

Huang, H., Ho, K.F., Lee, S.C., Tsang, P.K., Ho, S.S.H., Zou, C.W., Zou, S.C., Cao, J.J., Xu, H.M., 2012. Characteristics of carbonaceous aerosol in $PM_{2.5}$: Pearl Delta River Region, China. *Atmospheric Research* 104, 227–236.

Jiang, G.F., Fast, J.D., 2004. Modeling the effects of VOC and NO_x emission sources on ozone formation in Houston during the TexAQS 2000 field campaign. *Atmospheric Environment* 38, 5071–5085.

Kim, E., Hopke, P.K., 2004. Improving source identification of fine particles in a rural northeastern US area utilizing temperature–resolved carbon fractions. *Journal of Geophysical Research–Atmospheres* 109, art. no. D09204.

Kim, E., Hopke, P.K., Edgerton, E.S., 2003. Source identification of Atlanta aerosol by positive matrix factorization. *Journal of the Air & Waste Management Association* 53, 731–739.

Lam, K.S., Wang, T.J., Wu, C.L., Li, Y.S., 2005. Study on an ozone episode in hot season in Hong Kong and transboundary air pollution over Pearl River Delta region of China. *Atmospheric Environment* 39, 1967–1977.

Lamsal, L.N., Martin, R.V., Parrish, D.D., Krotkov, N.A., 2013. Scaling relationship for NO_2 pollution and urban population size: A satellite perspective. *Environmental Science & Technology* 47, 7855–7861.

Lee, T., Yu, X.Y., Ayres, B., Kreidenweis, S.M., Malm, W.C., Collett, J.L., 2008. Observations of fine and coarse particle nitrate at several rural locations in the United States. *Atmospheric Environment* 42, 2720–2732.

Li, S.M., Anlauf, K.G., Wiebe, H.A., Bottenheim, J.W., Shepson, P.B., Biesenthal, T., 1997. Emission ratios and photochemical production efficiencies of nitrogen oxides, ketones, and aldehydes in the Lower Fraser Valley during the Summer Pacific 1993 oxidant study. *Atmospheric Environment* 31, 2037–2048.

Liu, H., Wang, X.M., Zhang, J.P., He, K.B., Wu, Y., Xu, J.Y., 2013. Emission controls and changes in air quality in Guangzhou during the Asian Games. *Atmospheric Environment* 76, 81–93.

Nunnermacker, L.J., Imre, D., Daum, P.H., Kleinman, L., Lee, Y.N., Lee, J.H., Springston, S.R., Newman, L., Weinstein–Lloyd, J., Luke, W.T., Banta, R., Alvarez, R., Senff, C., Sillman, S., Holdren, M., Keigley, G.W., Zhou, X., 1998. Characterization of the Nashville urban plume on July 3 and July 18, 1995. *Journal of Geophysical Research–Atmospheres* 103, 28129–28148.

Paatero, P., Hopke, P.K., 2009. Rotational tools for factor analytic models. *Journal of Chemometrics* 23, 91–100.

Paatero, P., Hopke, P.K., Hoppenstock, J., Eberly, S.I., 2003. Advanced factor analysis of spatial distributions of $PM_{2.5}$ in the eastern United States. *Environmental Science & Technology* 37, 2460–2476.

Pandey, S.K., Tripathi, B.D., Mishra, V.K., Prajapati, S.K., 2006. Size fractionated speciation of nitrate and sulfate aerosols in a sub–tropical industrial environment. *Chemosphere* 63, 49–57.

Pathak, R.K., Chan, C.K., 2005. Inter–particle and gas–particle interactions in sampling artifacts of $PM_{2.5}$ in filter–based samplers. *Atmospheric Environment* 39, 1597–1607.

Pathak, R.K., Wang, T., Wu, W.S., 2011. Nighttime enhancement of $PM_{2.5}$ nitrate in ammonia–poor atmospheric conditions in Beijing and Shanghai: Plausible contributions of heterogeneous hydrolysis of N_2O_5 and HNO_3 partitioning. *Atmospheric Environment* 45, 1183–1191.

Pathak, R.K., Yao, X.H., Chan, C.K., 2004. Sampling artifacts of acidity and ionic species in $PM_{2.5}$. *Environmental Science & Technology* 38, 254–259.

Poirot, R.L., Wishinski, P.R., Hopke, P.K., Polissar, A.V., 2001. Comparative application of multiple receptor methods to identify aerosol sources in northern Vermont. *Environmental Science & Technology* 35, 4622–4636.

Polissar, A.V., Hopke, P.K., Poirot, R.L., 2001. Atmospheric aerosol over Vermont: Chemical composition and sources. *Environmental Science & Technology* 35, 4604–4621.

Raivonen, M., Vesala, T., Pirjola, L., Altimir, N., Keronen, P., Kulmala, M., Hari, P., 2009. Compensation point of NO_X exchange: Net result of NO_X consumption and production. *Agricultural and Forest Meteorology* 149, 1073–1081.

Roussel, P.B., Lin, X., Camacho, F., Laszlo, S., Taylor, R., Melo, O.T., Shepson, P.B., Hastie, D.R., Niki, H., 1996. Observations of ozone and precursor levels at two sites around Toronto, Ontario, during SONTOS 92. *Atmospheric Environment* 30, 2145–2155.

Seigneur, C., 2001. Current status of air quality models for particulate matter. *Journal of the Air & Waste Management Association* 51, 1508–1521.

Sillanpaa, M., Hillamo, R., Saarikoski, S., Frey, A., Pennanen, A., Makkonen, U., Spolnik, Z., Van Grieken, R., Branis, M., Brunekreef, B., Chalbot, M.C., Kuhlbusch, T., Sunyer, J., Kerminen, V.M., Kulmala, M., Salonen, R.O., 2006. Chemical composition and mass closure of particulate matter at six urban sites in Europe. *Atmospheric Environment* 40, S212–S223.

Sillman, S., 1995. The use of NO_Y, H_2O_2, and HNO_3 as indicators for ozone–NO_X–hydrocarbon sensitivity in urban locations. *Journal of Geophysical Research–Atmospheres* 100, 14175–14188.

Stehr, J.W., Dickerson, R.R., Hallock–Waters, K.A., Doddridge, B.G., Kirk, D., 2000. Observations of NO_Y, CO, and SO_2 and the origin of reactive nitrogen in the eastern United States. *Journal of Geophysical Research–Atmospheres* 105, 3553–3563.

Trainer, M., Parrish, D.D., Buhr, M.P., Norton, R.B., Fehsenfeld, F.C., Anlauf, K.G., Bottenheim, J.W., Tang, Y.Z., Wiebe, H.A., Roberts, J.M., Tanner, R.L., Newman, L., Bowersox, V.C., Meagher, J.F., Olszyna, K.J., Rodgers, M.O., Wang, T., Berresheim, H., Demerjian, K.L., Roychowdhury, U.K., 1993. Correlation of ozone with NO_Y in photochemically aged air. *Journal of Geophysical Research–Atmospheres* 98, 2917–2925.

Volz–Thomas, A., Berg, M., Heil, T., Houben, N., Lerner, A., Petrick, W., Raak, D., Patz, H.W., 2005. Measurements of total odd nitrogen (NO_Y) aboard MOZAIC in–service aircraft: Instrument design, operation and performance. *Atmospheric Chemistry and Physics* 5, 583–595.

Xiao, F., Brajer, V., Mead, R.W., 2006. Blowing in the wind: The impact of China's Pearl River Delta on Hong Kong's air quality. *Science of the Total Environment* 367, 96–111.

Xu, H.M., Tao, J., Ho, S.S.H., Ho, K.F., Cao, J.J., Li, N., Chow, J.C., Wang, G.H., Han, Y.M., Zhang, R.J., Watson, J.G., Zhang, J.Q., 2013. Characteristics of fine particulate non–polar organic compounds in Guangzhou during the 16th Asian Games: Effectiveness of air pollution controls. *Atmospheric Environment* 76, 94–101.

Zaveri, R.A., Berkowitz, C.M., Kleinman, L.I., Springston, S.R., Doskey, P.V., Lonneman, W.A., Spicer, C.W., 2003. Ozone production efficiency and NO_X depletion in an urban plume: Interpretation of field observations and implications for evaluating O_3–NO_X–VOC sensitivity. *Journal of Geophysical Research–Atmospheres* 108, art. no. 4436.

Zhang, S.J., Wu, Y., Liu, H., Wu, X.M., Zhou, Y., Yao, Z.L., Fu, L.X., He, K.B., Hao, J.M., 2013. Historical evaluation of vehicle emission control in Guangzhou based on a multi–year emission inventory. *Atmospheric Environment* 76, 32–42.

Zhang, J., Wang, T., Chameides, W.L., Cardelino, C., Kwok, J., Blake, D.R., Ding, A., So, K.L., 2007. Ozone production and hydrocarbon reactivity in Hong Kong, Southern China. *Atmospheric Chemistry and Physics* 7, 557–573.

Zheng, J.Y., Zhong, L.J., Wang, T., Louie, P.K.K., Li, Z.C., 2010. Ground–level ozone in the Pearl River Delta region: Analysis of data from a recently established regional air quality monitoring network. *Atmospheric Environment* 44, 814–823.